University of Baghdad
College of Engineering
JOURNAL OF ENGINEERING

Journal of Engineering

journal homepage: www.jcoeng.edu.iq

Volume 30 Number 5 May 2024

Structural Behavior Castellated 2C Cold-Formed Steel Beams

Mustafa Abdullah Gulam[1,*], Ahmad Jabbar Hussain Alshimmeri[2]

Department of Civil Engineering, College of Engineering, University of Baghdad, Baghdad, Iraq.
mustafa.gulam2001m@coeng.uobaghdad.edu.iq[1], dr.ahmadalshimmeri@coeng.uobaghdad.edu.iq[2]

ABSTRACT

This study's primary objective is to examine the structural behavior of using 2C-Cold produced. Section Castellated beams when subjected to monotonic load till failure. The experimental program testing. Seven Fabricated samples of castellated steel beams and one sample, which is a non-castellated steel beam (reference beam), were tested as supported beams under concentrated loads at two points over a clear span length (1730 mm). All castellated steel beams were similar in all properties and dimensions except the breadth of the upper and lower flanges. The current study considers the implications of modifying the width of the top and bottom flanges on how these beams behave. The findings showed that the ratio of the tested Castellated beams' ultimate load-carrying capacity to the non-castellated reference beam (R1) ranged from 99.3 to 117.2%, and the ratio of the tested beams' ultimate deflection to the same reference beam (R1) ranged from 72.6 to 103.2%. Increasing the breadth of the top and bottom flanges has a direct relationship with castellated beam stiffness and ultimate load. Finally, adjusting the flange width between the top and bottom flanges reduces castellated beam rigidity and ultimate load.

Keywords: Castellated steel beams, Flanges width, Cold-Formed steel, 2C-Channale.

*Corresponding author
Peer review under the responsibility of University of Baghdad.
https://doi.org/10.31026/j.eng.2024.05.10

Article received:04/07/2023
Article accepted: 11/10/2023
Article published: 01/05/2024

أداء العتبات الحديدية القلعوية ذات المقطع 2C المشكل على البارد

مصطفى عبد الله غلام*، احمد جبار حسين الشمري

قسم الهندسة المدنية، كلية الهندسة، جامعة بغداد، بغداد، العراق

الخلاصة

الهدف الرئيسي من هذا البحث هو دراسة السلوك الهيكلي لاستخدام العتبات المصقولة ذات المقطع البارد C2 عند تعرضها لحمل رتيب حتى الفشل. اختبار البرنامج التجريبي. تم اختبار سبع عينات مصنعة من العتبات الفولاذية المصقولة وعينة واحدة وهي العتبات الفولاذية غير المصقولة (العتبة المرجعية) كعتبات مدعمة ببساطة تحت أحمال مركزة عند نقطتين على طول امتداد واضح (1730 مم). كانت جميع العتبات الفولاذية المصقولة متشابهة في جميع الخصائص والأبعاد باستثناء عرض الحواف العلوية والسفلية. المعلمة الرئيسية التي تم أخذها في الاعتبار في العمل الحالي هي تأثيرات تغيير أبعاد عرض الحواف العلوية والسفلية في سلوك هذه العتبات. أظهرت النتائج أن نسبة القدرة التحملية النهائية للعتبات المخبرية المختبرة إلى العتبة المرجعية غير المحصنة (R1) تراوحت من 99.3 إلى 117.2%، ونسبة الانحراف النهائي للعتبات المختبرة إلى نفس العتبة المرجعية. (R1) تراوحت بين 72.6 إلى 103.2%. وتتناسب زيادة عرض الحواف العلوية والسفلية بشكل مباشر مع الصلابة والحمل النهائي للحزم المصقولة. وأخيرًا، فإن تبديل عرض الحافة بين الحواف العلوية والسفلية له تأثير ضئيل على الصلابة والحمل النهائي للحزم المصقولة.

الكلمات المفتاحية: عتبات حديدية قلعوية، عرض الشفة، حديد مشكل على البارد، قناة 2C .

1. INTRODUCTION

Castellated steel beams have become more common in the last 25 years. These days, design principles and comparatively well-established rules of practice control them, but they are always being updated to consider new information and results **(Fares, 2016)**. Castellated steel beams are one type of structural element. They are made by cutting a beam down the middle with a flame and then welding the two pieces together **(Tsavdaridis, 2015; Khaleel, 2021)**. This increases the total beam depth by 50% and strengthens the structure against bending **(Kerdal and Nethercot, 1984)**. Because of this, using these structural parts could save much money on materials **(Boyer,1964; Hadeed, 2019; Ammar and Alshimmeri, 2021; AL-Tameemi and Alshimmeri, 2023)**. Folding, press-braking of plates, or cold-rolling of coils manufactured from carbon steel are the three methods used to produce cold-formed steel sections. The sheet steel thickness in cold-formed sections is normally between 0.9 and 8 millimeters **(Zhu, 2017; Yu et al., 2019; Chen, 2020).** In compliance with European Standard EN 10142, it is often delivered to customers in a pre-galvanized state. Most cold-formed parts are very thin, so the thin plate parts tend to buckle locally when compressed **(Agapi, 2015; Craveiro, 2022)**. Local buckling of a cold-formed member typically entails plate flexure along a line of intersection of neighboring plates without any transverse deformation and may be characterized by a relatively small half-wavelength of the order of magnitude of individual plate components (**Martin et al., 2017**).

Cold-formed lipped channel beams (LCB) are often used as floor joists and bearers, which are parts that bend **(Mohsen and Mohammed, 2014; Said and Hashim, 2013; Al-Oukaili et al., 2013; Qassem, 2013; Mahmoud and Al-Janabi, 2014)**. The shear behavior of LCBs with web openings is more complicated, and the presence of web openings significantly reduces their shear capacities. It was studied how the cold-formed I-section castellated beam with different-sized cellular apertures and distance between openings **(Upadhyay, 2021)**. ABAQUS 6.13 is used to examine the performance while maintaining the section's depth and breadth constant. The Australian/New Zealand design code for cold-formed steel AS/NZS 4600:2005 and the North American specification for cold-formed steel AISI S-700:2007 are used in the theoretical investigation **(Hancock, 2008; Craveiro, 2022)**. A comparison and presentation of the outcomes anticipated by theoretical and numerical analysis are made. According to the data, the beam performs better when it has a cellular-shaped aperture that is 0.4 times the depth of the beam overall. Furthermore, the majority of castellated beams have been shown to collapse in their local failure modes. **(Chen et al., 2021)** examined fourteen beams with distinct whole spacing's and back-to-back channels that were put through four points of loading. Additionally, finite-element models were developed and verified by the trials. Following validation, a parametric analysis utilizing 63 FEMs looked at the effects of fillet radius, stiffener length, beam length, and whole diameter on the findings. The tests' findings demonstrate that, compared to a plain channel, the moment capacity of two adjacent channels with five edge-stiffened holes rose by 15.4%. The same segment with the reinforced holes had a 15.1% reduced moment capacity. The test results also demonstrate that each case cracked often due to buckling. **(Roy et al., 2021)** examined the findings from twelve experiments. Two distinct cross-sections, referred to as BU75 and BU90, were taken into consideration, with screw spacings of 1900 mm, 950 mm, and 475 mm. The initial geometric faults were measured before the bending testing. Next, a nonlinear elastoplastic FE model was created, and the outcomes of it and the test results agreed rather well. In a comprehensive parametric investigation, the impact of screw spacing on the flexural strength of such back-to-back built-up CFS channel beams was examined using the validated FE model. The outcomes of 108 parametric analyses are presented in total. When the FE model and test data were compared, there was good agreement in terms of failure mechanisms and flexural capabilities. The American Iron and Steel Institute (AISI) and Australian Standard's (AS) design strengths were compared to the experimental and FE findings. **(Amayreh et al., 2012; Gholizadeh et al., 2011; MR et al., 2012; Keerthika, 2020)** examined a particular steel segment; castellated beams are manufactured with increased web opening depth. Beams are subjected to experimental testing under two-point loads and supported conditions. The central beam deflection and different failure patterns are explored. The depth-increasing beams and the parent section are compared based on various characteristics and serviceability criteria. Many investigations on the structural behavior of castellated steel beams have resulted from their extensive usage as structural members. Castellated beams are effective for moderately loaded and longer spans when deflection controls the design. From the experimental testing, it can be inferred that the castellated steel beam is serviceable up to a maximum opening depth of 0.6D. (**Al-Mawashee and Al-Kannoon, 2021**) conducted an experiment on four beams of identical length (1.7 m) subjected to a single point load at midspan. The two castellated beams under investigation have similar step lengths for their castellation and corrugation profiles, corrugated webs, and lateral stiffeners or not. The primary variable for castellated-corrugated web beams is whole beam height. The maximum load capacity of castellated-corrugated web beams is higher than that of plain and corrugated web beams.

The results demonstrate that the load capacities of flat and corrugated web beams are greater than those of castellated-corrugated web beams, with (23.7%, 39.4%) and (13.2%, 31.03%), respectively. They investigated the structural behavior of 2c-cold formed section castellated beams when subjected to monotonic load until failure. The investigation focused on determining how the changing dimensions of the top and bottom flanges affected the results.

This paper collected a considerable amount of information during the testing, and discrepancies and peculiarities were highlighted and discussed. The structural behavior of the eight tested specimens (seven double-channel castellated steel beams and the non-castellated beam) was observed and discussed in terms of their relationship to ultimate yield and service states, load-deflection, the failure mode, deflection profiles, and load strains of steel. The results of two reference beams (a non-castellated beam and a Castellated beam) were always used as a reference beam for comparison purposes. They were tested as supported beams under concentrated loads at two points over a clear span length (1730 mm) and total length (1930 mm).

2. EXPERIMENTAL PROGRAM AND MATERIAL PROPERTIES

2.1 Tested Steel Beams

The experimental program involves seven Fabricated samples of castellated steel beams and one sample, which is a non-castellated steel beam (reference beam). The key parameter considered in the present work is the effects of changing dimensions of the top and bottom flanges' widths influence the behavior of a 2C cold-formed castellated steel beam. Double cold-formed castellated steel channel sections were manufactured from (2) mm thick steel plates and then linked back-to-back using bolts and flange welding, resulting in a single beam consisting of composite parts. The samples were first cut to the proper proportions and then hooked in the shape of the letter C with a crimping machine. All beams were evaluated as supported beams under focused loads at two points throughout a clear span length (1730 mm) and total length (1930 mm). **Fig. 1** shows the details of the non-castellated steel beam (reference beam).

All castellated steel beams were similar in all properties and dimensions except the top and bottom flanges' widths. **Fig. 2** shows the profile of the castellated beams, while **Figs. 3 to 9** show the sections in these beams. **Table 1** shows the parametric details of the tested steel beams.

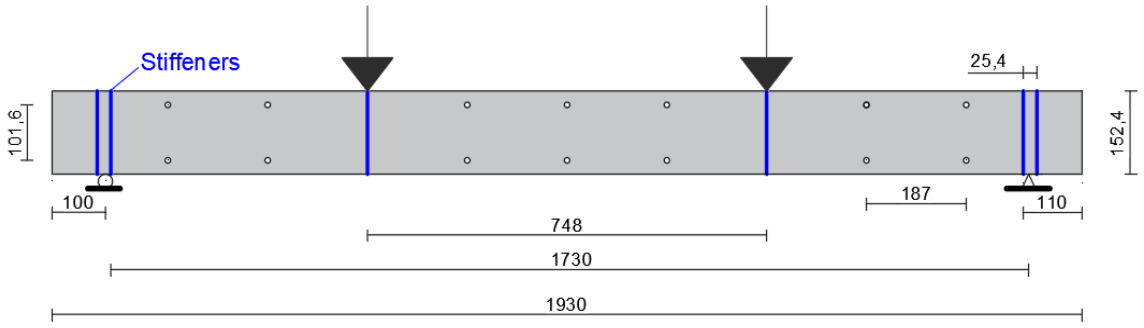

(a)

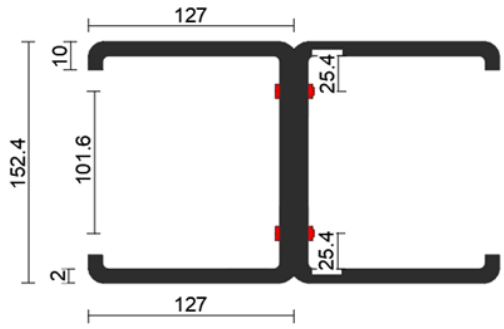

(b)

Figure 1. Details of the reference beam (BT5B5R1) (a) Beam, and (b) Section (all dimensions are in millimeters)

Table 1. Details of tested beams

Specimen ID	Beam type	The width of the upper flange(mm)	The width of the bottom flange(mm)
BT5B5R1	Solid	5 (127)	5 (127)
CBT2B5	castellated	2 (50.8)	5 (127)
CBT3B5	castellated	3 (76.2)	5 (127)
CBT4B5	castellated	4 (101.6)	5 (127)
CBT5B5R2	castellated	5 (127)	5 (127)
CBT5B2	castellated	5 (127)	2 (50.8)
CBT5B3	castellated	5 (127)	3 (76.2)
CBT5B4	castellated	5 (127)	4 (101.6)

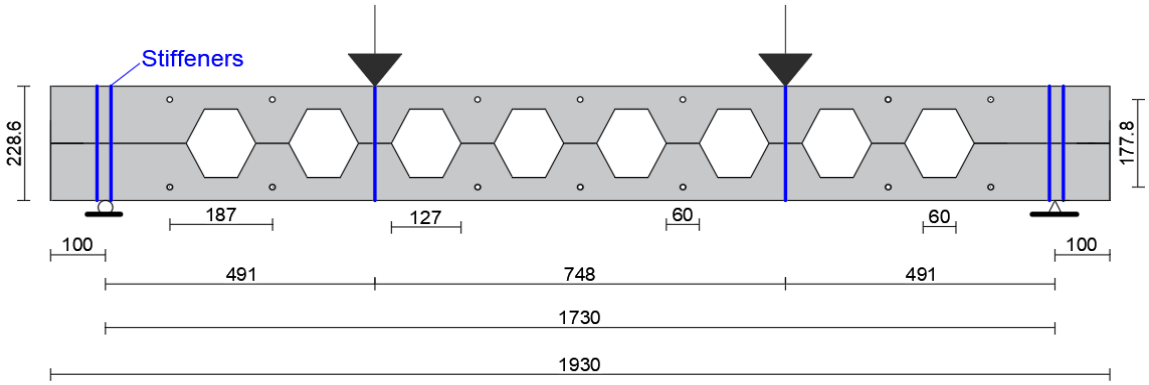

Figure 2. Details of the castellated beams

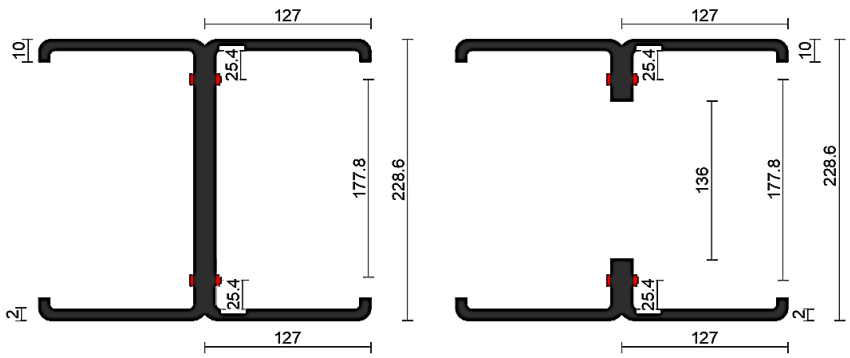

a-Section at web post b-Section at opening

Figure 3. Details of the castellated beam reference two CBT5B5R2

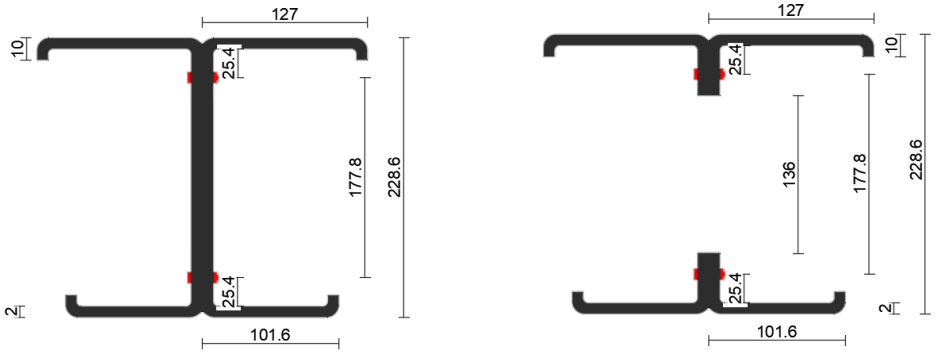

a-Section at web post b-Section at opening

Figure 4. Details of the castellated beam CBT5B4

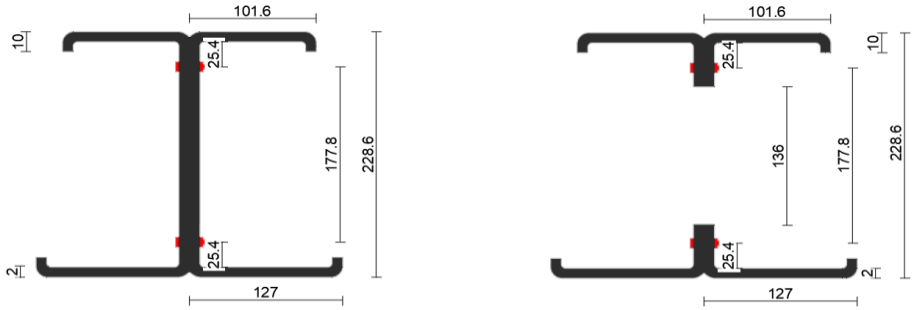

a-Section at web post b-Section at opening

Figure 5. Details of the castellated beam CBT4B5

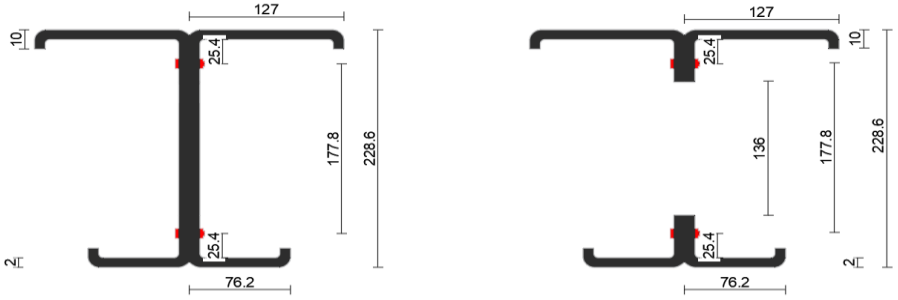

a-Section at web post b-Section at opening

Figure 6. Details of the castellated beam CBT5B3

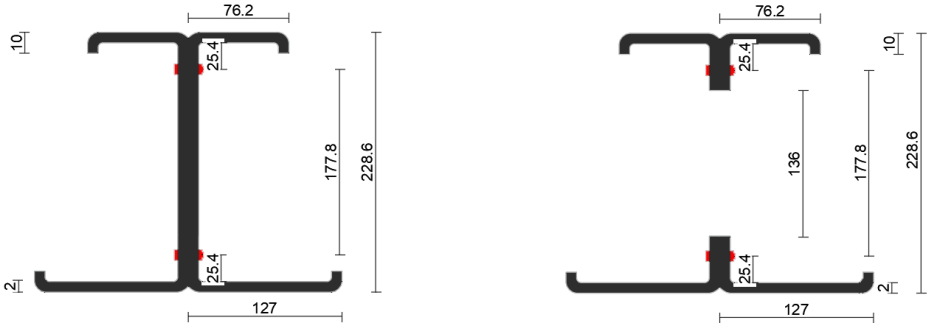

a-Section at web post b-Section at opening

Figure 7. Details of the castellated beam CBT3B5

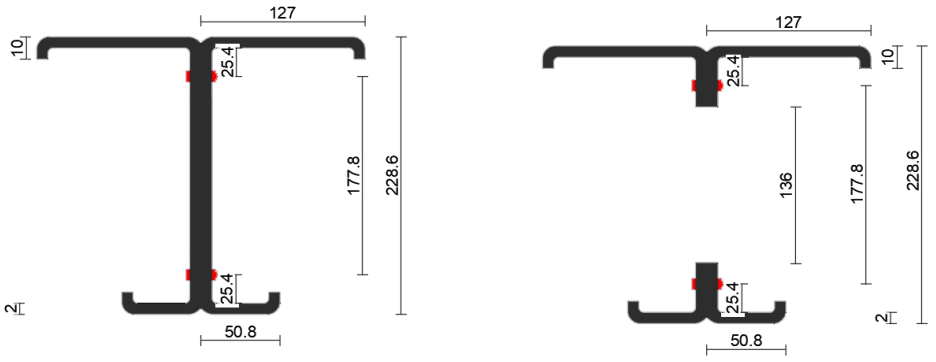

a-Section at web post b-Section at opening

Figure 8. Details of the castellated beam CBT5B2

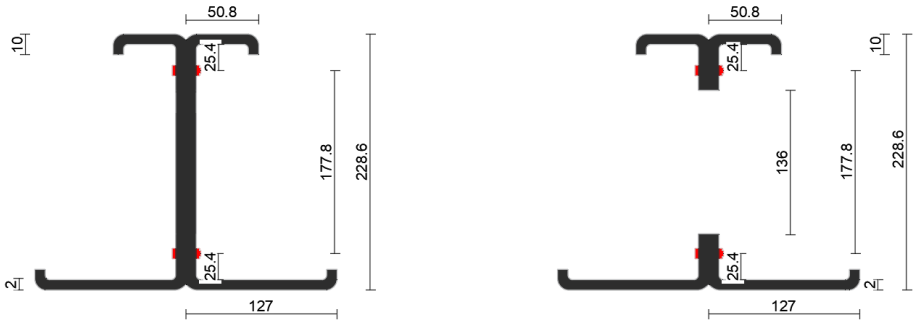

a-Section at web post b-Section at opening

Figure 9. Details of the castellated beam CBT2B5

***(all dimensions are in mm)**

2.2 Materials Properties

The qualities of steel plate were the thickness 2mm, yield stresses 378 MPa, Ultimate stresses 478 MPa and Elongations test value 30%, and ASTM specifications specify elongation limits greater than or equal to 10%. Furthermore, coupon piece samples from each web and flanges were cut and tested according to (**ASTM A370, 2006**) To determine the mechanical characteristics of the steel section. **Fig. 10** shows the dimensions of the coupon piece.

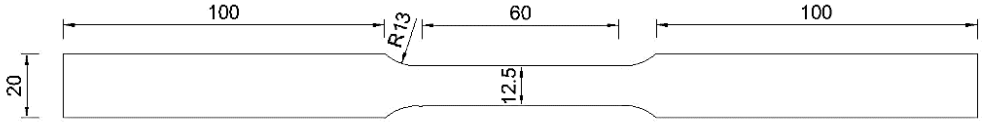

Figure 10. Steel plate coupon samples (all dimensions are in mm), **(ASTM A370, 2006)**

Laboratory tests were performed at the University of Baghdad's consulting office. The steel plate used for the beam's sections and stiffeners in this paper had a thickness of 2 mm.
Steel stiffeners made from the same plate a thickness of 2 mm were used to achieve the strengthening approach, as shown in **Figs. 11. and 12** shows the beam test setup.

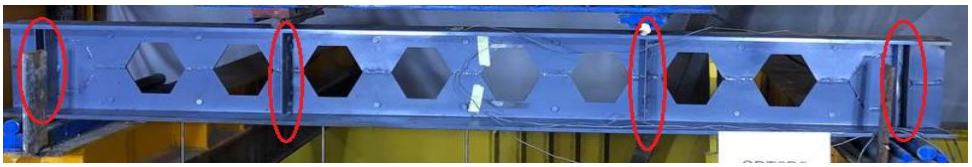

Figure 11. Position of stiffeners

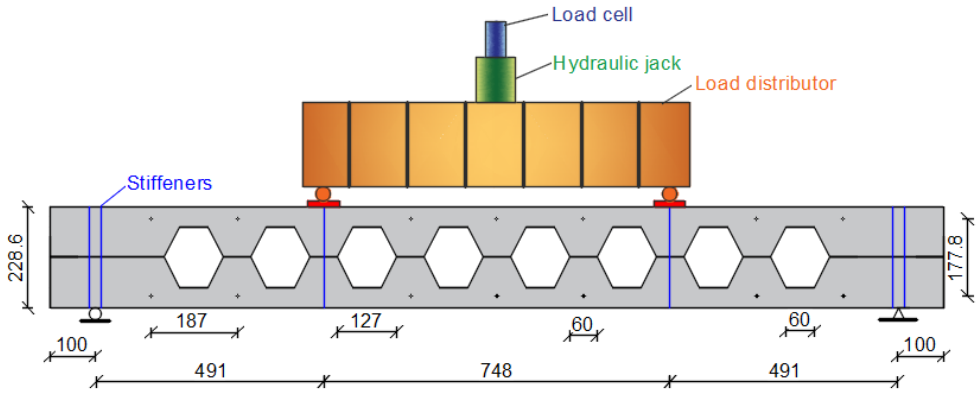

Figure 12. Beam test setup

3. RESULTS AND DISCUSSION

3.1 Ultimate, yield and service states

Results of the ultimate state are shown in **Tables 2 and 3**, while the results of the yield state are shown in **Tables 4** and **5**. Finally, the results of the surface state are shown in **Tables 6 and 7. Fig. 13** shows the tested beams' ultimate load, yield, and service load capacity. The tested beams' ultimate load-carrying capacity ranged from 99.3 to 117.2% when compared to the non-castellated reference beam (R1), and their ultimate deflection ranged from 72.6 to 103.2% when compared to the same reference beam (R1). The tested beams' ultimate load-carrying capacity ranged from 84.7 to 97.6% when compared to the castellated reference beam (R2), and their ultimate deflection ranged from 88.2 to 125.5% when compared to the same reference beam (R2).

The examined beams' yield load ratio to the non-castellated reference beam (R1) varied between 96.9 and 112.3%, while their yield deflection ratio to the same reference beam (R1) varied between 80 and 93.3%. The examined beams' yield load ratio to the castellated reference beam (R2) varied between 86.3 and 97.3%, while their yield deflection ratio to the same reference beam (R2) varied between 99.7 and 124.6%.

There was a range of 99 to 117.2% for the service load ratio of the tested beams compared to the non-castellated reference beam (R1), and 68.8 to 102.5% for the service deflection ratio of the same reference beam (R1). The examined beams' service load to castellated reference beam (R2) ratios varied from 84.7 to 97.6%, while their service deflection to the same reference beam (R2) ratios varied from 104 to 149.1%. The width and size of flanges can have a significant impact on the ultimate, yield, and service states when the chosen serviceability limit was 60% of the experimental ultimate load. In general, the examined beams' maximum load-bearing capability was directly correlated with their flange width. The highest value of the ultimate load-carrying capacity of the castellated reference beam

(CBT5B5R2), whose flange widths are 5 inches on both the top and bottom, makes it suitable for 2C cold-formed castellated beams.

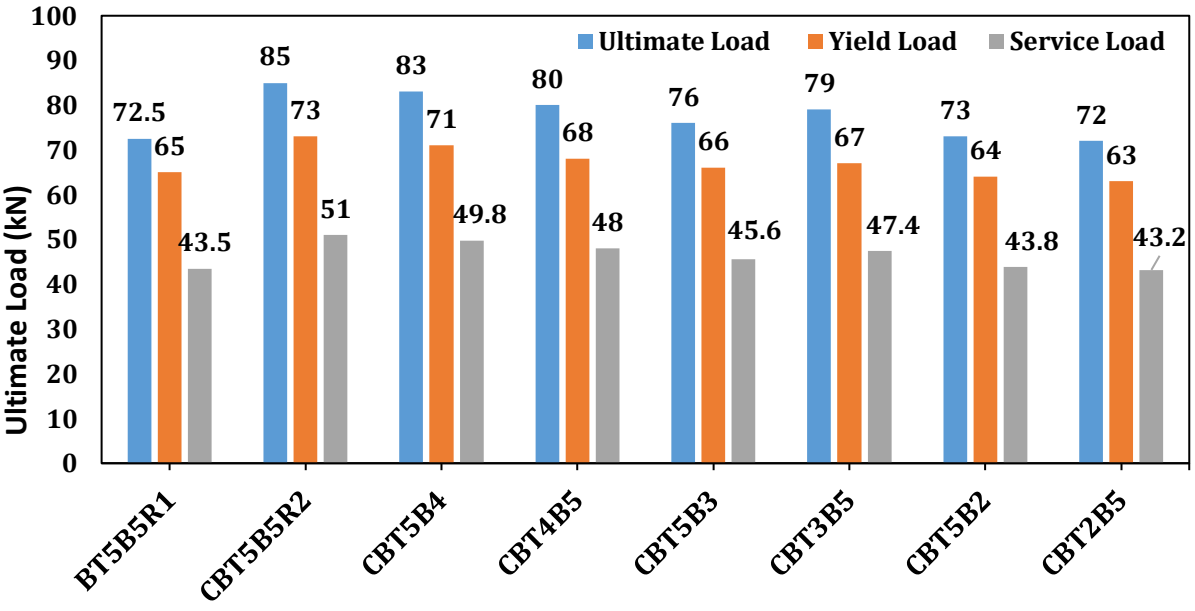

Figure13. Ultimate load, yield load, and service load capacity for tested specimens

Table2. A comparison of the ultimate state concerning the non-castellated reference beam (R1)

ID of the Specimen	Ultimate Load Pu (kN)	The ultimate load's deflection (Δu) (mm)	$Pu/ Pu_{ref.} \times 100$ (%)	$\Delta u/\Delta u_{ref.} \times 100$ (%)
BT5B5R1	72.5	6.2	Ref.	Ref.
CBT5B5R2	85	5.1	117.2	82.3
CBT5B4	83	6.4	114.5	103.2
CBT4B5	80	6.1	110.3	98.4
CBT5B3	76	5.6	104.8	90.3
CBT3B5	79	6.11	108.9	98.5
CBT5B2	73	5.5	100.7	88.7
CBT2B5	72	4.5	99.3	72.6

Table 3. A comparison of the ultimate state concerning the castellated reference beam (R2)

ID of the Specimen	Ultimate Load Pu(kN)	The ultimate load's deflection (Δu) (mm)	$Pu/ Pu_{ref.} \times 100$ (%)	$\Delta u/\Delta u_{ref.} \times 100$ (%)
CBT5B5R2	85	5.1	Ref.	Ref.
BT5B5R1	72.5	6.2	85.3	121.6
CBT5B4	83	6.4	97.6	125.5
CBT4B5	80	6.1	94.1	119.6
CBT5B3	76	5.6	89.4	109.8
CBT3B5	79	6.11	92.9	119.8
CBT5B2	73	5.5	85.9	107.8
CBT2B5	72	4.5	84.7	88.2

Table 4. A comparison of yield state concerning the non-castellated reference beam (R1)

ID of the Specimen	Yield Load Py (kN)	Deflection at yield load (Δy) (mm)	$Py/ Py_{ref.} \times 100$ (%)	$\Delta y/\Delta y_{ref.} \times 100$ (%)
BT5B5R1	65	4.61	Ref.	Ref.
CBT5B5R2	73	3.7	112.3	80.3
CBT5B4	71	3.69	109.2	80
CBT4B5	68	3.8	104.6	82.4
CBT5B3	66	3.92	101.5	85
CBT3B5	67	3.88	103.1	84.2
CBT5B2	64	4.3	98.5	93.3
CBT2B5	63	4.14	96.9	89.8

Table 5. A comparison of yield state concerning the castellated reference beam (R2)

ID of the Specimen	Yield Load Py (kN)	Deflection at yield load (Δy) (mm)	$Py/ Py_{ref.} \times 100$ (%)	$\Delta y/\Delta y_{ref.} \times 100$ (%)
CBT5B5R2	73	3.7	Ref.	Ref.
BT5B5R1	65	4.61	89	124.6
CBT5B4	71	3.69	97.3	99.7
CBT4B5	68	3.8	93.2	102.7
CBT5B3	66	3.92	90.4	105.9
CBT3B5	67	3.88	91.8	104.9
CBT5B2	64	4.3	87.7	116.2
CBT2B5	63	4.14	86.3	111.9

Table 6. A comparison of service state concerning the non-castellated reference beam (R1)

ID of the Specimen	Service Load Ps (kN)	At service load, deflection (Δs) (mm)	$Ps/ Ps_{ref.} \times 100$ (%)	$\Delta s/\Delta s_{ref.} \times 100$ (%)
BT5B5R1	43.5	3.2	Ref.	Ref.
CBT5B5R2	51	2.2	117.2	68.8
CBT5B4	49.8	2.29	114.5	71.6
CBT4B5	48	2.51	110.3	78.4
CBT5B3	45.6	2.86	104.8	89.4
CBT3B5	47.4	2.7	109	84.4
CBT5B2	43.8	3.15	100.7	98.4
CBT2B5	43.2	3.28	99	102.5

Table 7. A comparison of service state concerning the castellated reference beam (R2)

ID of the Specimen	Service Load Ps (kN)	At service load, deflection (Δs) (mm)	$Ps/ Ps_{ref.} \times 100$ (%)	$\Delta s/\Delta s_{ref.} \times 100$ (%)
CBT5B5R2	51	2.2	Ref.	Ref.
BT5B5R1	43.5	3.2	85.3	145.5
CBT5B4	49.8	2.29	97.6	104
CBT4B5	48	2.51	94.1	114
CBT5B3	45.6	2.86	89.4	130
CBT3B5	47.4	2.7	92.9	122.7
CBT5B2	43.8	3.15	85.9	143.2
CBT2B5	43.2	3.28	84.7	149.1

3.2 Load-Deflection Behavior

The tested beams' load-deflection characteristics is shown in **Figs. 14 and 15**. The load-deflection relationship may be described in three stages, as follows. At the first stages of loading, it was observed that deflection increased almost linearly up to the advanced stage of loading. In the second stage, the deflections were more apparent from the start of loading. As a result, the slope of the load-deflection curves before the peak was non-linear. At the third stage (after the peak), the deflections increased with a decrease in load.
Fig. 14 shows that the castellated reference beam (CBT5B5R2) with width of 5 inches for top and bottom flanges was stiffer than the non-castellated reference beam (BT5B5R1) with the same width of top and bottom flanges, that's because the increasing of the total specimen depth and moment of inertia of the starting beam (BT5B5R1), where the ultimate load of castellated reference beam (CBT5B5R2) increased by 17.2% concerning the starting beam (BT5B5R1). **Figs. 15 to 17** show that switching the width of the flange between the top and bottom flanges has relatively little impact on the stiffness and ultimate load of castellated beams. **Fig. 18** shows that increasing the top and bottom flanges' width is directly proportional to the stiffness and ultimate load of castellated beams.

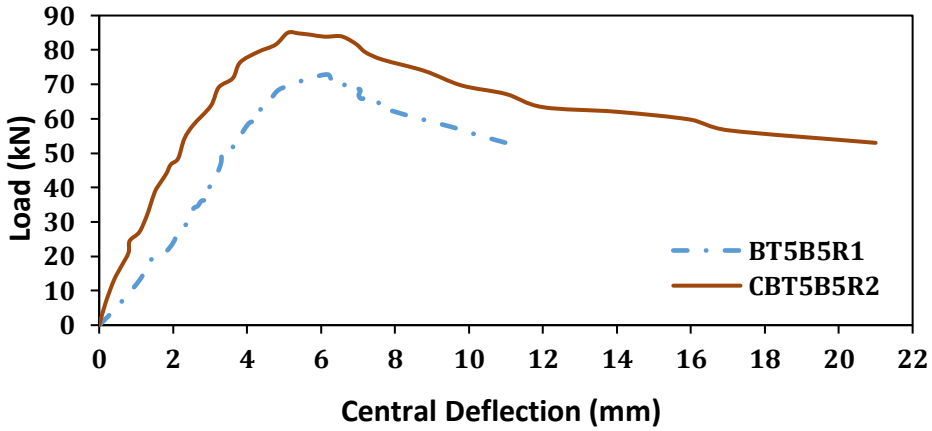

Figure 14. Load-deflection relationships of reference beams

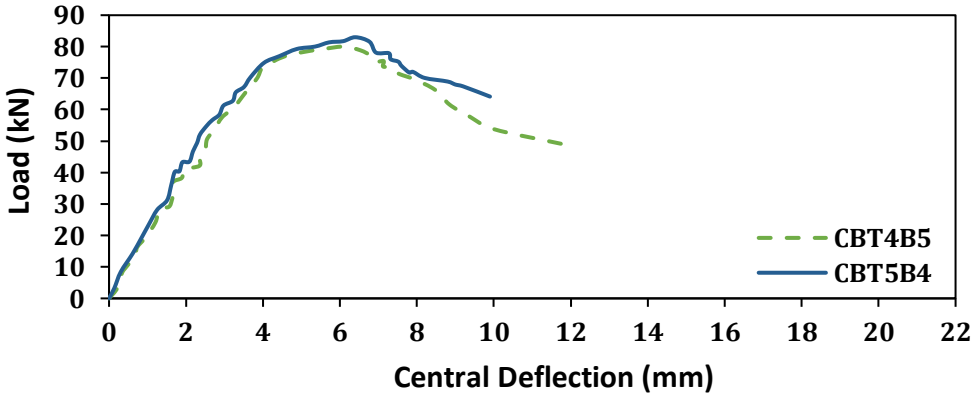

Figure 15. Load-deflection relationships of beams CBT5B4 and CBT4B5

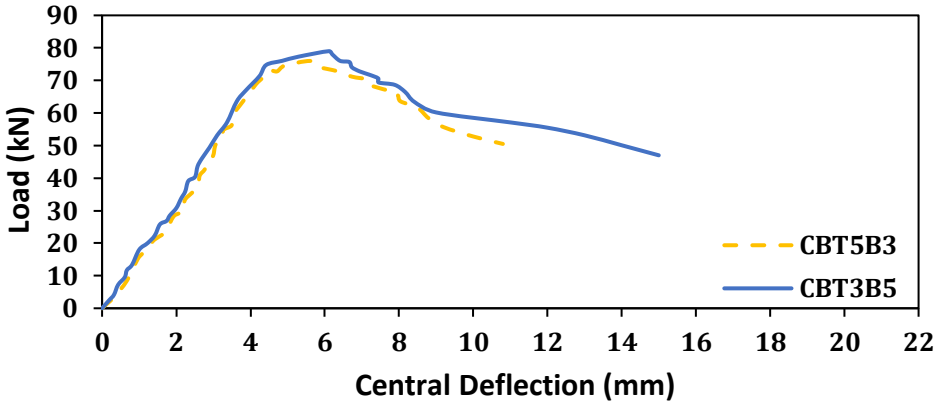

Figure 16. Load-deflection relationships of beams CBT5B3 and CBT3B5

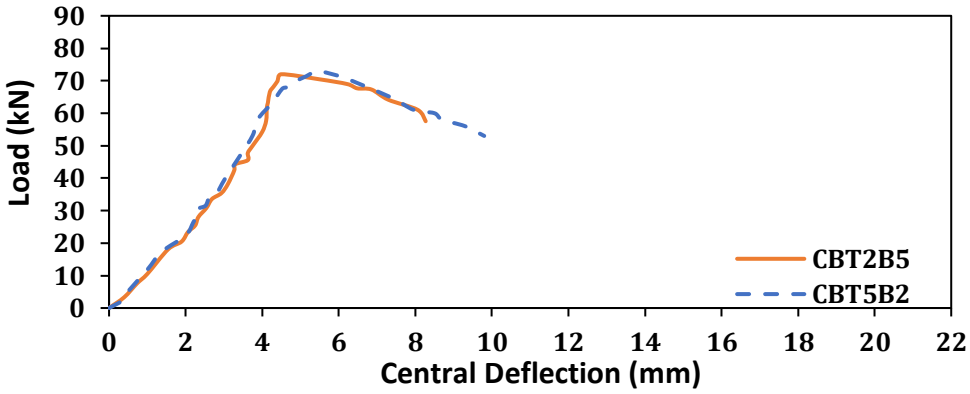

Figure 17. Load-deflection relationships of beams CBT5B2 and CBT2B5

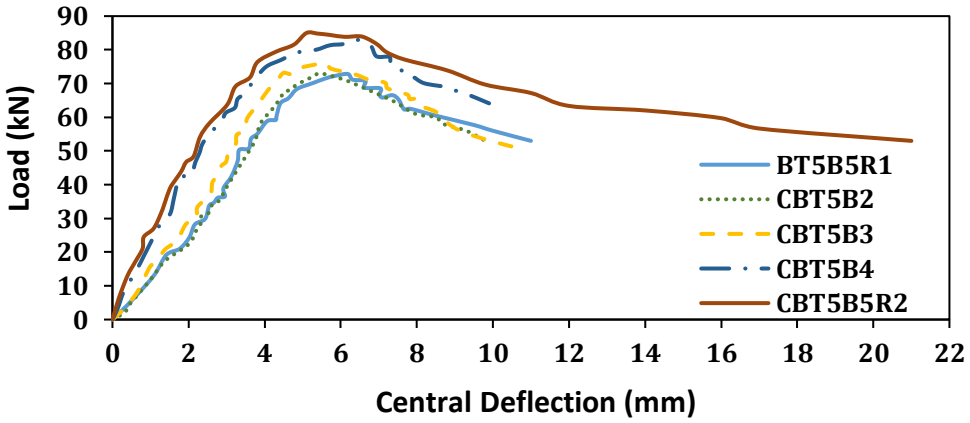

Figure 18. Load-deflection relationships of beams with different widths of flange

Table 8 summarizes the relevant mid-span deflections at the minimum ultimate load of the tested beams (CBT2B5). The chosen load is important to compare deflections at a constant load as an indicator of the stiffness of beams.

At load of 72 KN, the mid-span deflection decreases by 36.5, 31.6, 31.2, 20.5, 24, 6.7, and 21% for CBT5B5R2, CBT5B4, CBT4B5, CBT5B3, CBT3B5, CBT5B2, and CBT2B5 respectively concerning the non-castellated reference beam (BT5B5R1). It is evident that the stiffness of castellated beams is directly proportional to the width of the top and bottom flanges, and that the stiffness of castellated beams is only little affected by the flange width that is switched between the top and bottom flanges.

Table 8. Beam deflection as a function of load, at load =72 KN

Specimen ID	At 72 KN	
	Deflection (mm)	Decreasing in deflection (%)
BT5B5R1	5.7	Ref.
CBT5B5R2	3.62	36.5
CBT5B4	3.9	31.6
CBT4B5	3.92	31.2
CBT5B3	4.53	20.5
CBT3B5	4.33	24
CBT5B2	5.32	6.7
CBT2B5	4.5	21

3.3 Deflection Profile

Deflections along the tested beams at the center of the first post, the center of the third hole, and the mid-span beam have been measured at three loading stages (30, 50 kN, and ultimate load), as demonstrated in **Figs. 19 to 26**. This deflection primarily occurred at the sections between the posts (openings portions), as shown by the steep decline in rafter stiffness across these sections, which is best seen at the first post next to the support because this region is the closest point to the support. These diagrams also show how the holes affected the moment of inertia, causing the curves to be composed of curved segments. The maximum beam deflection may be determined using the beam deflection profile.

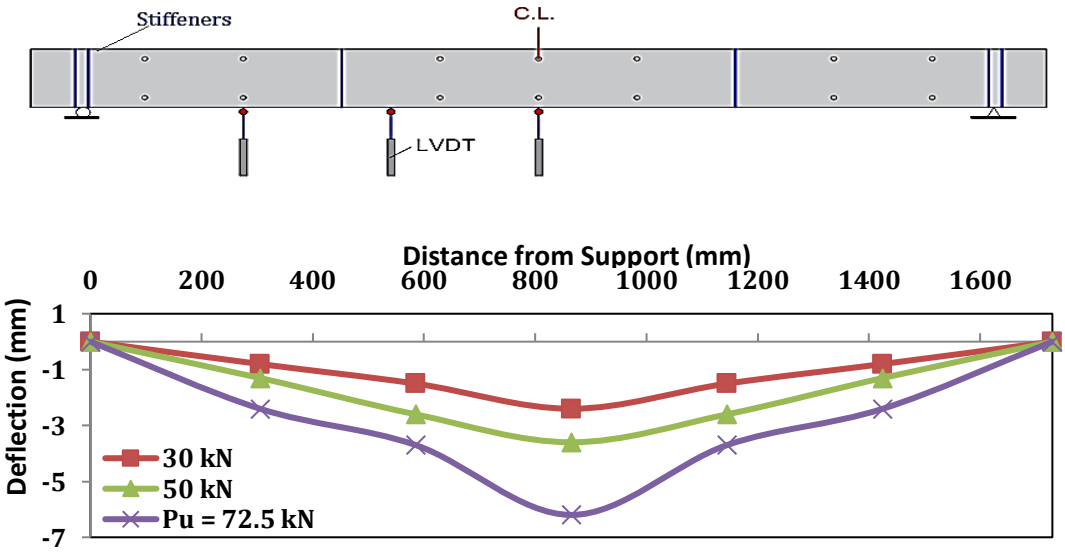

Figure 19. Deflection profile of the beam BT5B5R1

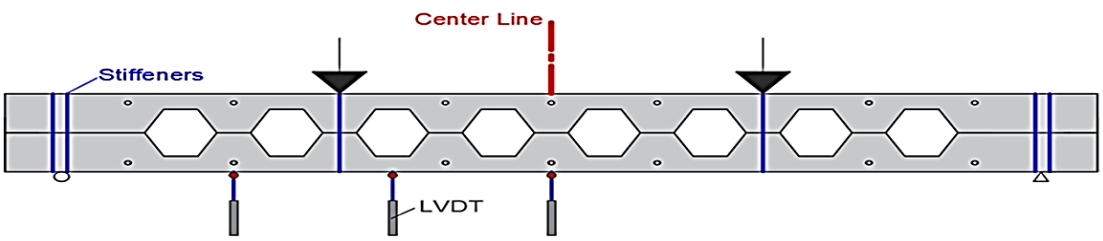

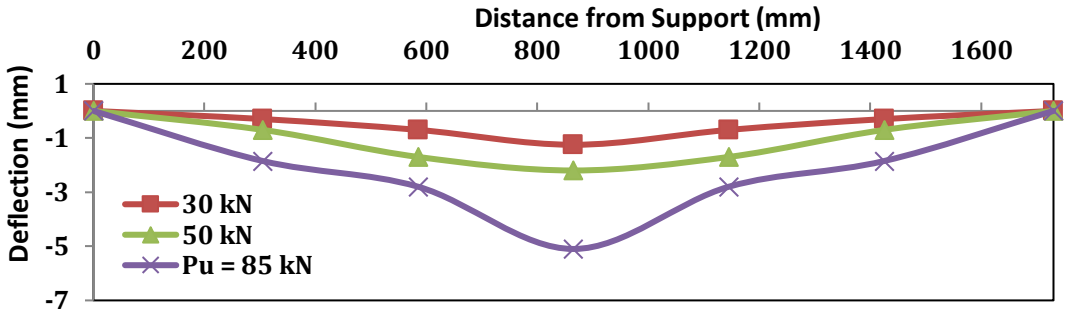

Figure 20. Deflection profile of the beam CBT5B5R2

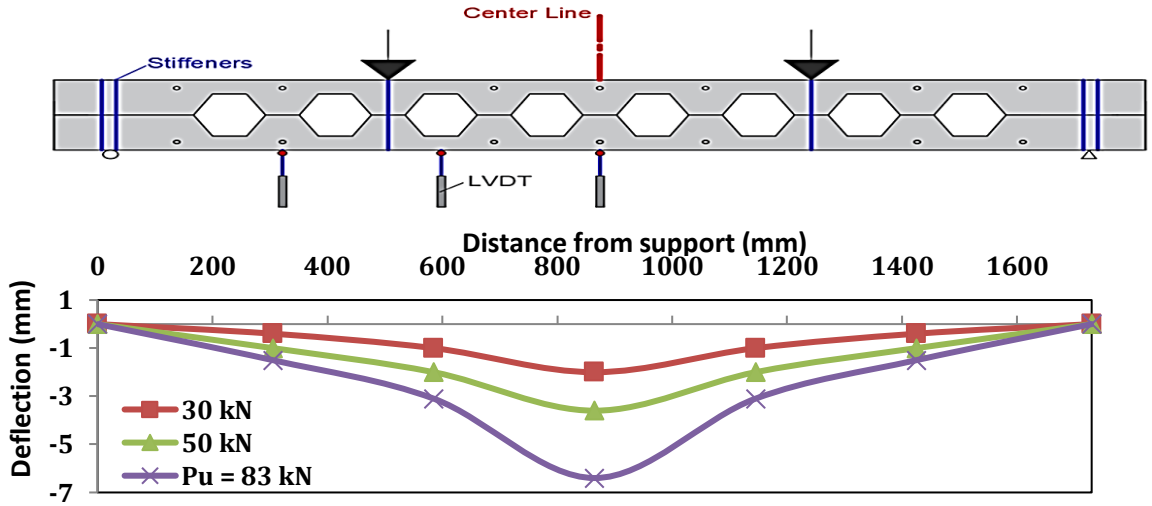

Figure 21. Deflection profile of the beam CBT5B4

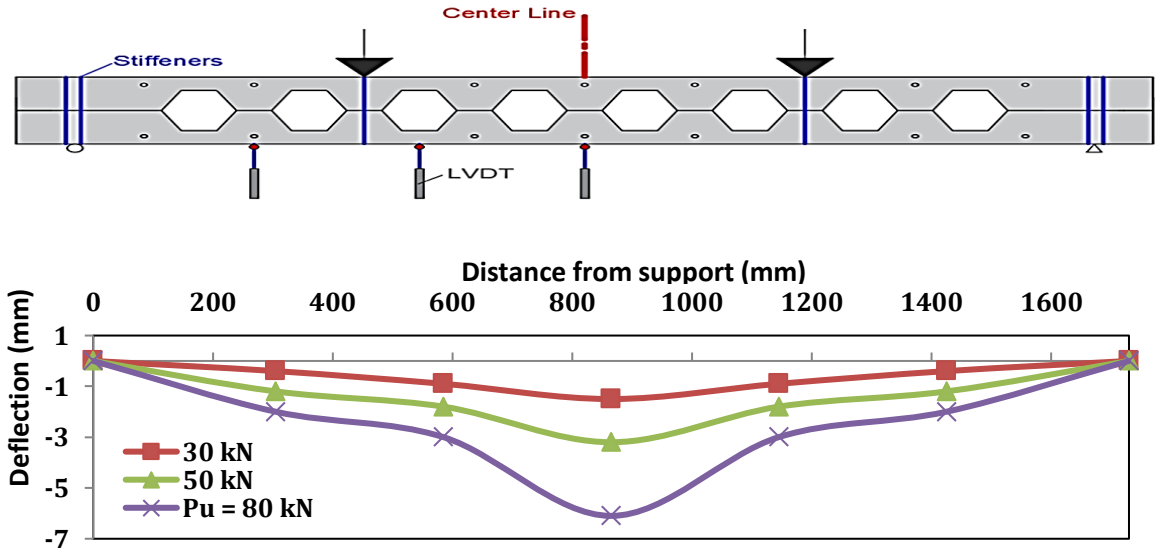

Figure 22. Deflection profile of the beam CBT4B5

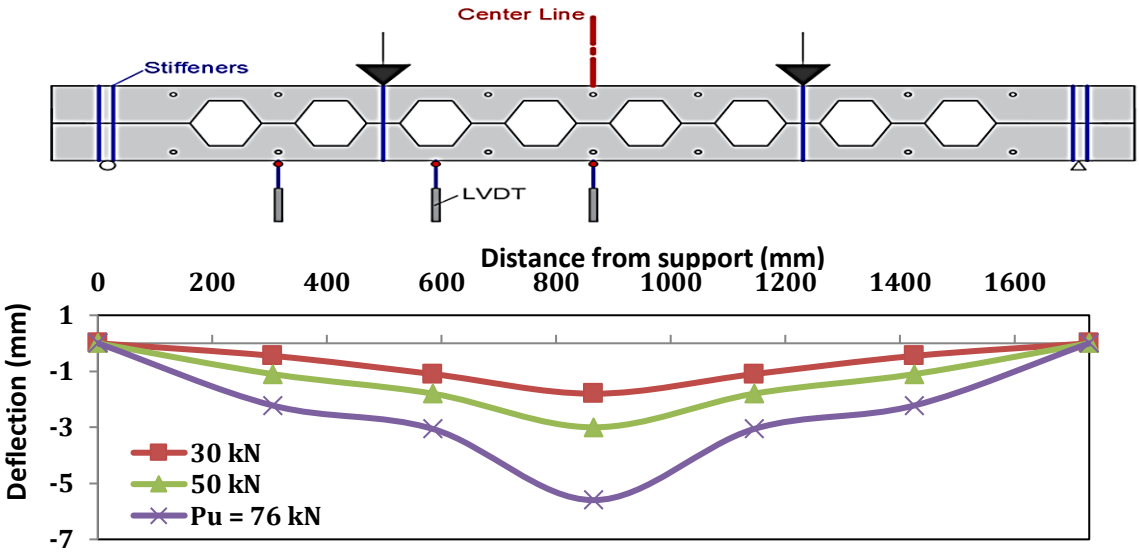

Figure 23. Deflection profile of the beam CBT5B3

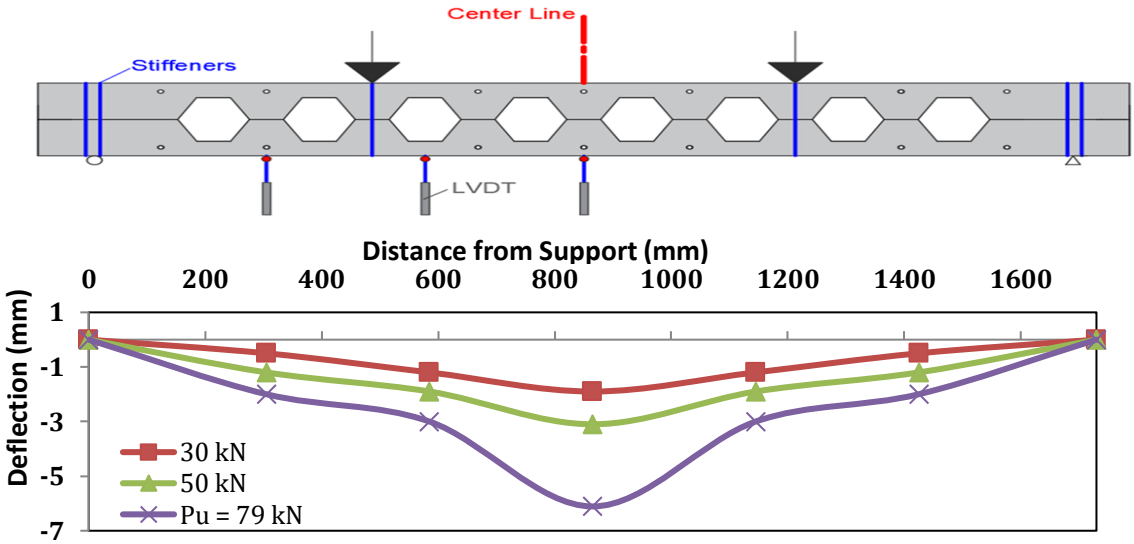

Figure 24. Deflection profile of the beam CBT3B5

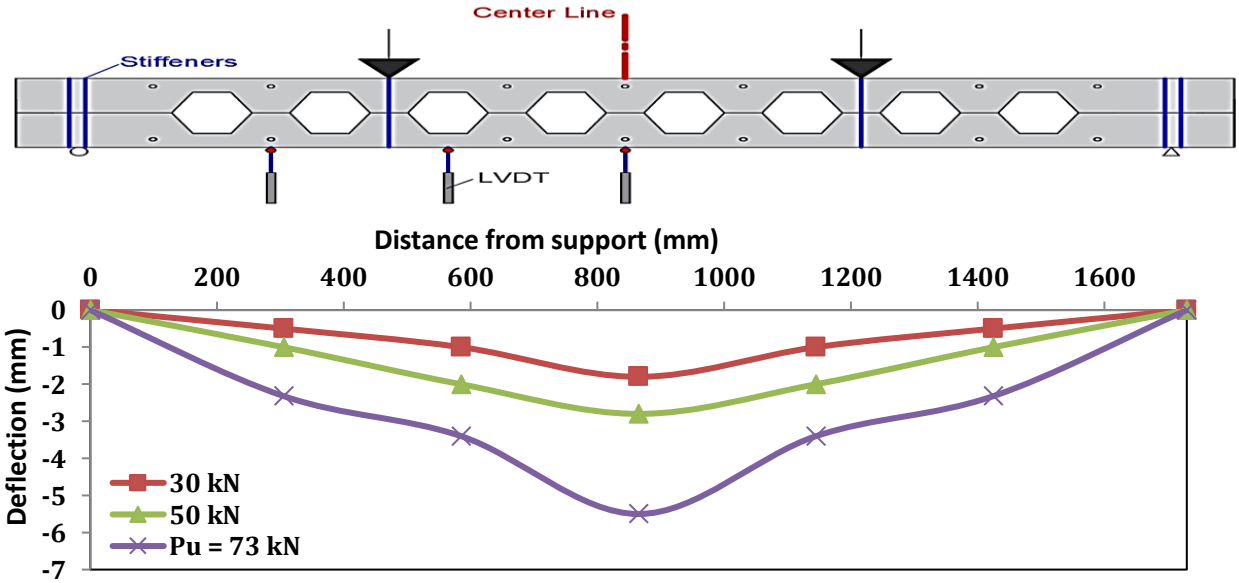

Figure 25. Deflection profile of the beam CBT5B2

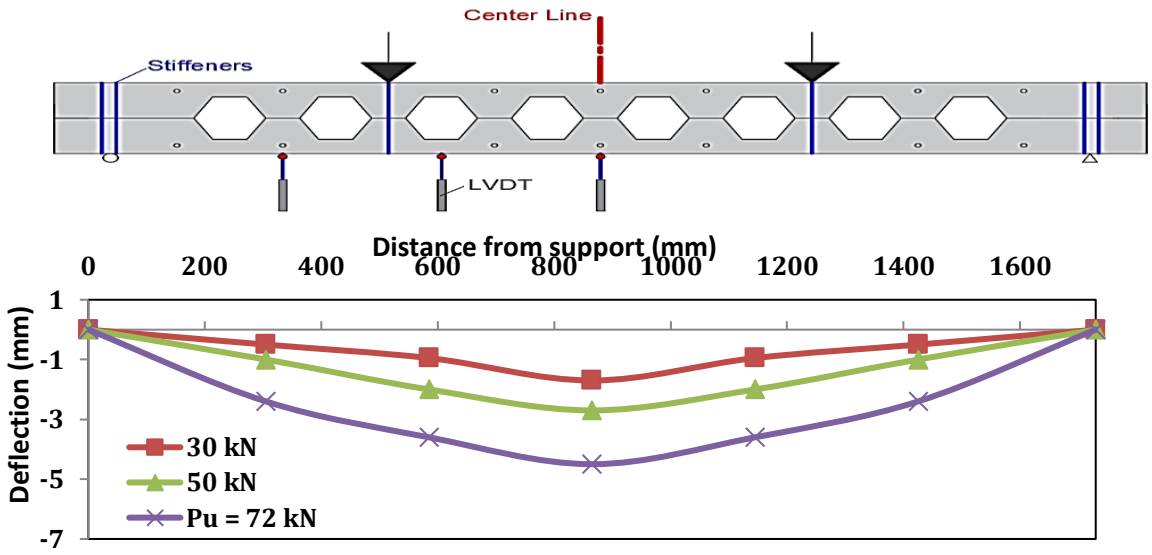

Figure 26. Deflection profile of the beam CBT2B5

3.4 Modes of Failure

This paper defines the failure load as the equivalent of the highest applied static load, beyond which the beam exhibited a significant reduction in strength and finally failed. Certain failure modes are specific to castellated beams, such as failure (Vierendeel), buckling for a web post, web weld fracture, and flexural mechanism. etc., have been recognized as a consequence of the various series of tests achieved in several countries. Moreover, the connection failures are associated with the built-up section. Contrarily, failure modes for the castellated beams were varied. For example, as shown in **Figs. 28, 33, and 34**, respectively, a Vierendeel failure mode was developed in the three beams CBT5B5R2, CBT3B5, and CBT5B4**. (Altifillisch, 1957; Toprac and Cooke, 1959; Kerdal, 1984)** describes the castellated beam's Vierendeel failure type. Such a disaster was caused by a large shear force placed on the beam. **(Wang, 2014)**. All of which had flanges with a different width. A Vierendeel mode may have occurred due to the stress concentration at the corners of the holes producing the formation of plastic hinges **(Mali, 2023),** (as an approach of the parallelogram). Beam BT5B5R1 exhibits an overall flexure mechanism. This breakdown happens in the area that has a significant bending moment.

This failure style was documented in the writings of **(Halleux, 1967)**, and compression flange local Buckling, as shown in **Fig. 27**. This kind of fiasco is happened by the response point or center load subordinate immediately to web post, this fiasco can be forbidden by using suitable reinforcement stiffeners to web **(Husain and Speirs, 1973)**. **Table 9** summarizes the failure mode for all tested specimens. Beams CBT5B3 and CBT4B5 exhibit Web post Buckling and local compression flange Buckling. At the same time, beam CBT5B2 shows a local compression flange Buckling. Beam CBT2B5 exhibits a local tension flange Buckling and local compression flange Buckling. Finally, CBT3B5 and CBT5B4 exhibit the rupture of the welding joint, local Buckling in compression flange, and Vierendeel as shown in **Figs. 33 and 34**. The welding joint burst According to research by, if the welded joint's length is short, the horizontal shear stress is high and causes the beam to rupture. **(Husain and Speirs, 1971)**.

Table 9. The failure mode of beams.

Specimen ID	*Modes of Failure*
BT5B5R1	Overall flexure mechanism and local Buckling in compression flange
CBT5B5R2	Vierendeel, local Buckling in compression flange, and rupture of the welding
CBT5B3	Web post Buckling and local Buckling in compression flange
CBT4B5	Web post Buckling and local Buckling in compression flange
CBT5B2	local Buckling in compression flange
CBT2B5	local Buckling in tension flange and local Buckling in compression flange
CBT3B5	The rupture of the welding joint, local Buckling in compression flange, and Vierende
CBT5B4	The rupture of the welding joint, local Buckling in compression flange, and Vierende

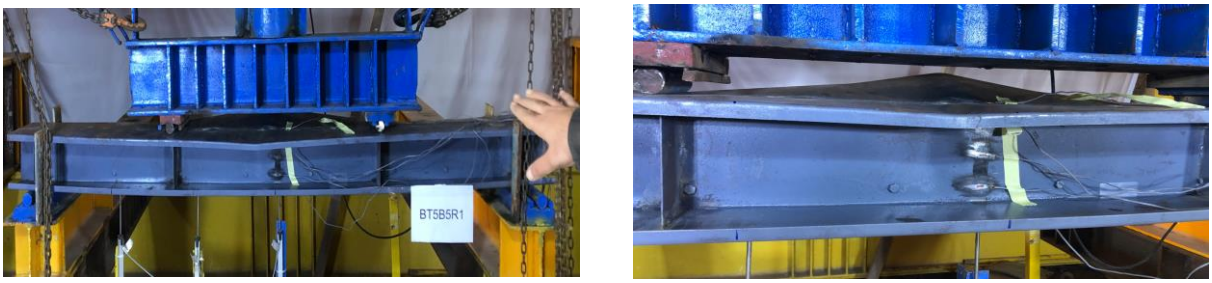

Figure 27. Failure modes of beam BT5B5R1

Figure 28. Failure modes of beam CBT5B5R2

Figure 29. Failure modes of beam CBT5B3

Figure 30. Failure modes of beam CBT4B5

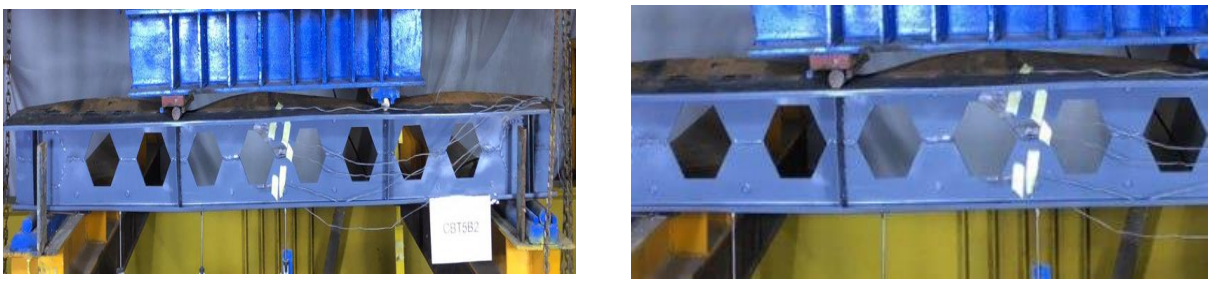

Figure 31. Failure modes of beam CBT5B2

Figure 32. Failure modes of beam CBT2B5

Figure 33. Failure modes of beam CBT3B5

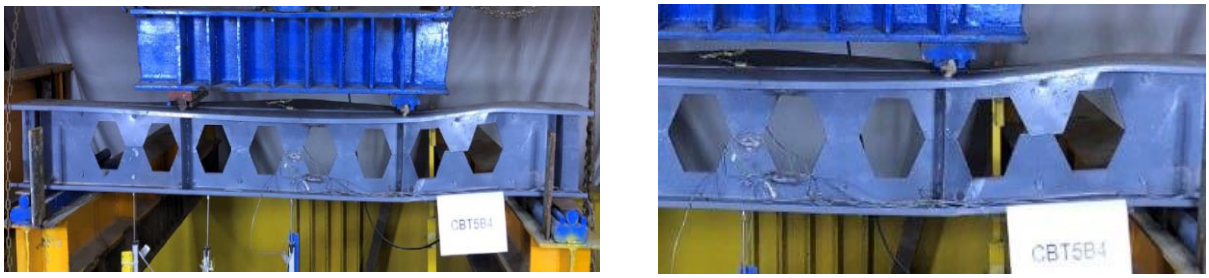

Figure 34. Failure modes of beam CBT5B4

4. CONCLUSIONS

The main aim of this thesis is to investigate the demeanor of double-channel castellated cold steel beams. A further The purpose of this article is to create a finite element model to aid in future research on the analysis of castellated steel beams under static loads. The findings of this inquiry are as follows:-

1. The ultimate load-carrying capacity of the tested beams to the non-castellated reference beam (R1) ranged from 99.3 to 117.2%, and the ratio of the ultimate deflection of tested beams to the same reference beam (R1) ranged from 72.6 to 103.2%, While the loads for the reference load (R2) ranged from 84.7 to 97.6%, and the ultimate deflection ranged from 88.2 to 125.5%.

2. The yield load of the tested beams to the non-castellated reference beam (R1) ranged from 96.9 to 112.3%, and the ratio of the yield deflection of tested beams to the same reference beam (R1) ranged from 80 to 93.3%, However, the percentage was from 86.3 to 97.3% for the revised reference threshold (R2), and the yield deviation ratio for the same threshold (R2) ranged from 99.7 to 124.6%.
3. The service load of the tested beams to the non-castellated reference beam (R1) ranged from 99 to 117.2%, and the ratio of the service deflection of tested beams to the same reference beam (R1) ranged from 68.8 to 102.5%, However, the percentage of service loads relative to the reference threshold (R2) ranged from 84.7 to 97.6%, while the deviation for the same threshold (R2) ranged from 104 to 149.1%
4. Increasing the width of the top and bottom flanges is directly proportional to the stiffness and ultimate load of castellated beams.
5. The castellated reference beam (CBT5B5R2) with a width of 5 inches for top and bottom flanges was stiffer than the non-castellated reference beam (BT5B5R1) with the same top and bottom flanges width. That is because of the increase of the total specimen depth and moment of inertia of the starting beam (BT5B5R1), where the ultimate load of castellated reference beam (CBT5B5R2) increased by 17.2% concerning the starting beam (BT5B5R1).
6. Switching the flange width hardly affects the stiffness between the top and bottom flanges and ultimate load of castellated beams.

Acknowledgements

This work was funded by the (Department of Civil Engineering, College of Engineering, University of Baghdad). The authors would like to thank the staff at the Department of Electrical Engineering. This job could not be completed without their assistance and contributions.

Credit Authorship Contribution Statement

Dr. Ahmed Jabbar Hussain Alshimmeri wrote the initial text, while Mustafa Abdullah Gulam wrote the review and editing, validation, and conceptualization.

Declaration of Competing Interest

The authors state that they have no known conflicting financial interests or personal ties that might have influenced the work presented in this study.

REFERENCES

Al-Mawashee, H.S., and Al-Kannoon, M.A., 2021. Flexural strength of castellated beams with corrugated webs. *Journal of Physics: Conference Series*. Vol. 1973. No. 1. IOP. Doi:10.1088/1742-6596/1973/1/012213

Al-Oukaili, N.K., Al-Zaidee, S.R., and Al Mallah, N. M., 2013. The Use of Bracing Dampers in Steel Buildings under Seismic Loading. *Journal of Engineering*, 19(9), pp. 1094-1101. Doi:10.31026/j.eng.2013.09.04

Al-Tameemi, S.K., and Alshimmeri, A.J., 2023. Behavior of asymmetrical castellated composite girders by gap in steel web. *AIP Conference Proceedings*. (Vol. 2414, No. 1). AIP Publishing. Doi:10.1063/5.0116809

Altifillisch, M. D., Cooke, R. B., and Toprac, A. A., 1957. *An investigation of open web expanded beams*. Welding Research Council Bulletin, New York, 47, pp. 307-320

Agapi, A.M., 2015. *Finite element analysis of lapped connections between cold formed steel purlins* (Universitat Politècnica de Catalunya).

Ammar, H.A., and Alshimmeri, A.J.H., 2021. A Comparison Study between Asymmetrical Castellated Steel Beams Encased by Reactive Powder Concrete with Laced Reinforcement. *Key Engineering Materials*, 895(6), pp. 77-87. Doi:10.4028/www.scientific.net/kem.895.77

Amayreh, L., and Saka, M. P., 2005. Failure Load Prediction of Castellated Beams Using Artificial Neural Networks. *Asian Journal of Civil Engineering (Building and Houseing)*, 6, pp. 33-54

ASTM A370, 2006. Standard Testing Method and Definitions for Steel Products, ASTM Designation A 370, ASTM international, Pennsyl Vania, United State. www.astm.org/astm-tpt-724.html

Boyer, J.P.,1964. Castellated Beam-New Development. AISC National Engineering Conference, AISC Engineering Journal, 3, pp. 106-108. https://www.aisc.org/Castellated-Beams-New-Developments

Chen, B., Roy, K., Fang, Z., Uzzaman, A., Raftery, G. and Lim, J.B., 2021. Moment capacity of back-to-back cold-formed steel channels with edge-stiffened holes, un-stiffened holes, and plain webs. *Engineering Structures*, *235*, p.112042. Doi:10.1016/j.engstruct.2021.112042

Chen, M.T., and Young, B., 2020. Tests of cold-formed normal and high strength steel tubes under tension. *Thin-Walled Structures*, 153, P.106844. Doi:10.1016/j.tws.2020.106844

Craveiro, H.D., Rahnavard, R., Laím, L., Simões, R.A., and Santiago, A., 2022. Buckling behavior of closed built-up cold-formed steel columns under compression. *Thin-Walled Structures*, 179, P.109493. Doi:10.1016/j.tws.2022.109493

Fares, S., Coulson, J., and Dinehart, D., 2016. Castellated and cellular beam design. American Institute of Steel Construction

Hadeed, S.M., and Alshimmeri, A.J.H., 2019. Comparative Study of structural behavior for rolled and castellated steel beams with different strengthening techniques. *Civil Engineering Journal*, 5(6), pp. 1384-1394. Doi:10.28991/cej-2019-03091339

Halleux, P., 1967. Limit analysis of castellated steel beams. *Acier-Stahl-Steel*, *32*(3), pp.133-144.

Hancock, G.J., 2008. Development of the 2005 Edition of the Australian/New Zealand Standard for Cold-Formed Steel Structures AS/NZS 4600. *Advances in Structural Engineering*, 11(6), pp. 585-597

Hosain, M., and Spiers, W., 1973. *Experiments on castellated steel beams*. American Welding Society, Welding Research Supplement, 52(8), pp. 329S-342

Husain, M., and Spiers, W., 1970. Failure of Castellated Beams due to Rupture of Welded Joints. Acier-Stahl-Steel, 36(1), pp. 34-40

Keerthika, V. and Daniel Thangaraj, D., 2020. Numerical Analysis on Load Carrying Capacity of Castellated Beam by Varying Web Opening. In *Indian Structural Steel Conference* (pp. 527-540). Singapore: Springer Nature Singapore. Doi:10.1007/978-981-19-9390-9_42

Kerdal, D., and Nethercot, D.A. 1984. Failure Modes for Castellated beams. *Journal of Constructional Steel Research*, 4, pp. 295-315. Doi:10.1016/0143-974x(84)90004-x

Khaleel, A.I.و and AL-Shamaa, M.F., 2021. Experimental Investigation on the Structural Behavior of Double Channel Castellated Steel Beams. In E3S Web of Conferences (Vol. 318, P. 03009). EDP Sciences. Doi:10.1051/e3sconf/202131803009

Mahmoud, T.K. and Al-Janabi, M.A.Q., 2014. Behavior of Spliced Steel Girders under Static Loading. *Journal of Engineering*, *20*(10), pp.93-109. Doi:10.31026/j.eng.2014.10.07

Mali, S.S. and Kumbhar, P.D., 2024. Comparative study on behaviour of castellated beams with diamond-and hexagonal-shaped openings using CFRP stiffeners. *Asian Journal of Civil Engineering*, *25*(1), pp.939-952. Doi:10.1007/s42107-023-00823-x

Martin, Lawrence, and John Purkiss., 2017. Structural Design of Steelwork to EN 1993 and EN 1994. CRC Press. Doi:10.1201/b12852

Mohsen, M. H., and Mohammed, S. N., 2014. The effective width in composite steel concrete beams at ultimate loads. *Journal of Engineering*, *20*(8), pp. 1-17. Doi:10.31026/j.eng.2014.08.01

MR, W., AV, S. and Auti, V.A., 2012. Parametric study of castellated beam with varying depth of web opening. *International journal of scientific and Research publications*, *287*.

Qassem, Z. S., 2013. Load Distribution Factors for Horizontally Curved Composite Concrete-Steel Girder Bridges. *Journal of Engineering*, *19*(2), pp. 167-179. Doi:10.31026/j.eng.2013.02.01

Roy, K., Lau, H.H., Ting, T.C.H., Chen, B., and Lim, J.B., 2021, February. Flexural behaviour of back-to-back built-up cold-formed steel channel beams: Experiments and finite element modelling. *Structures*, 29, pp. 235-253. Doi:10.1016/j.istruc.2020.10.052

Said, A. I., and Hashim, I. H., 2013. Analysis and optimum design of self supporting steel communication tower. *Journal of Engineering*, *19*(12), pp. 1673-1687. Doi:10.31026/j.eng.2013.12.14

Toprac, A., and Cooke, B., 1959. *The plastic behavior of castellated beams*. Welding Research Council Bulletin, New York, 47, pp. 1-10

Tsavdaridis, K.D., Kingman, J.J. and Toropov, V.V., 2015. Application of structural topology optimisation to perforated steel beams. *Computers & structures*, *158*, pp.108-123. Doi:10.1016/j.compstruc.2015.05.004

Upadhyay, M.H., Patel, V.B. and Arekar, V.A., Parametric study on castellated beam with arch-shape openings. *SSRG International Journal of Civil Engineering*, 8(5), pp. 52-57. Doi:10.14445/23488352/ijce-v8i5p106

Wang, P., Ma, Q. and Wang, X., 2014. Investigation on Vierendeel mechanism failure of castellated steel beams with fillet corner web openings. Engineering structures, 74, pp.44-51. Doi:10.1016/j.engstruct.2014.05.008

Yu, W.W., LaBoube, R.A. and Chen, H., 2019. *Cold-formed steel design*. John Wiley & Sons.

Zhu, A., Zhang, X., Zhu, H., Zhu, J., and Lu, Y., 2017. Experimental study of concrete filled cold-formed steel tubular stub columns. *Journal of Constructional Steel Research*, 134, pp. 17-27. Doi:10.1016/j.jcsr.2017.03.003